sciendo

POLISH MARITIME RESEARCH 1 (117) 2023 Vol. 30; pp. 98-111
10.2478/pomr-2023-0010

HIERARCHICAL MULTISCALE FLUCTUATION DISPERSION ENTROPY FOR FUEL INJECTION SYSTEM FAULT DIAGNOSIS

Qingguo Shi
Yihuai Hu*
Guohua Yan
Shanghai Maritime University, China

* Corresponding author: *yhhu@shmtu.edu.cn (Yihuai Hu)*

ABSTRACT

Marine electronically controlled (ME) two-stroke diesel engines occupy the highest market share in newly-built ships and its fuel injection system is quite different and important. Fault diagnosis in the fuel injection system is crucial to ensure the power, economy and emission of ME diesel engines, so we introduce hierarchical multiscale fluctuation dispersion entropy (HMFDE) and a support matrix machine (SMM) to realise it. We also discuss the influence of parameter changes on the entropy calculation's accuracy and efficiency. The system simulation model is established and verified by Amesim software, and then HMFDE is used to extract a matrix from the features of a high pressure signal in a common rail pipe, under four working conditions. Compared with vectorised HMFDE, the accuracy of fault diagnosis using SMM is nearly 3% higher than that using a support vector machine (SVM). Experiments also show that the proposed method is more accurate and stable when compared with hierarchical multiscale dispersion entropy (HMDE), hierarchical dispersion entropy (HDE), multiscale fluctuation dispersion entropy (MFDE), multiscale dispersion entropy (MDE) and multiscale sample entropy (MSE). Therefore, the proposed method is more suitable for the modelling data. This research provides a new direction for matrix learning applications in fault diagnosis in marine two-stroke diesel engines.

Keywords: Hierarchical multiscale fluctuation dispersion entropy; fuel injection system; support matrix machine; fault diagnosis

INTRODUCTION

With the characteristics of high thermal efficiency, high power, long service life, and easy maintenance, diesel engines play an important role in transportation, agriculture, industry, national defence and other fields [1]. According to relevant statistics, 90% of marine ships use diesel engines as their main propulsion units. However, marine diesel engines generally use low-quality heavy fuel oil [2,3], which will produce a large number of nitrogen oxides, sulphur oxides, carbon dioxide, particulate matter, volatile organic compounds, oily sewage and other hazards. These have become the main source of pollutants in the sea and coastal areas of ports, causing serious damage to the ecological environment and affecting people's health [4]. The fuel injection system of a marine diesel engine has an important influence on its power, economy and emissions [5], such as improving combustion performance, reducing pollutant emissions and increasing diesel engine power [6]. The ideal fuel injection system has the characteristics of high injection pressure, flexible adjustment of the injection law and injection timing [7]. Low emissions, low fuel consumption, high reliability, large degree of control freedom and convenient operation and maintenance are the goals pursued by the continuous development of marine diesel engines. Because of their high control accuracy, great flexibility and complete functionality, electronic fuel injection systems have greatly improved the fuel economy of diesel engines and reduced pollutant emissions, which has become

a research hotspot in the diesel engine industry, both at home and abroad, and is an inevitable trend of the development of marine diesel engines [8].

At present, low-speed marine diesel engines mainly include marine electronically controlled (ME) diesel engines produced by MAN Company and RT-Flex diesel engines produced by the WinGD Corporation. According to statistics in Shanghai, China, ME type diesel engines have the highest market share, with an average of 56%, as shown in Table 1. The fuel injection system of an ME diesel engine is electronically controlled, with the characteristics of high injection pressure, flexible adjustment of injection law, injection timing and injection pressure. It is also the largest contributing factor to diesel engine failure [9]. Therefore, fault diagnosis in the fuel injection system of an ME two-stroke diesel engine is of great significance.

Tab. 1. Statistics of types of diesel engines used on newly-built ships in Shanghai, China.

Years	Number of newly built ships	Number of marine electronically controlled diesel engines	Number of dual fuel diesel engines
2019	26	17	1
2020	24	13	8
2021	41	21	12

The existing fault diagnosis method for diesel engines is widely based on the vibration signal. Wang et al. [10] measured the cylinder head surface vibration signals under three conditions of a diesel engine: normal state, injection advance angle leading and injection advance angle lagging, and used adaptive wavelet packets and EEMD fractal dimensions for fault diagnosis. Krogerus et al. [11] identified the injection duration of pilot diesel injectors by measuring the high pressure common rail fuel pipe pressure vibration signal of a dual fuel diesel engine. Yang et al. [12] collected the vibration signals of a diesel engine surface under seven common valve faults, and adopted a combination of the discriminative non-negative matrix factorisation (DNMF) and the KNN classifier. Desbazeille et al. [13] analysed the crankshafts' angular speed variations to monitor the working condition of a large diesel engine. Liu et al. [14] proposed a novel fault diagnosis method for diesel engines based on self-adaptive WVD, improved FCBF and a relevance vector machine (RVM); the results demonstrated that the method can effectively extract the relevant fault features and can accurately identify the fault types. From the above research, we see that most of these experiments were carried out in a laboratory environment, which lacks interference, and the vibration signal is more susceptible to noise pollution. The working environment is harsher, especially for a marine two-stroke diesel engine which generates a higher possibility of interference from vibration data. Cherednichenko et al. [15] undertook the physical modelling of thermochemical fuel treatment processes. Varbanets et al. [16] pointed out that mathematical simulation of the engine was helpful in identifying malfunctions and predicting the effects of a malfunction on the performance of the engine. Zhao et al. [17] used numerical simulations and experimental tests to evaluate the effects of different hydrogen ratios on the combustion and emissions of diesel engines. In order to obtain more abundant diesel engine data, Rodriguez et al. [18] obtained diesel engine data through a computational fluid dynamics model under several pre-injection patterns. Gupta et al. [19] presented the modelling and control of a novel pressure regulation mechanism for the common rail fuel injection system of internal combustion engines and validated it by using Amesim software. Some researchers also used the Amesim software to build a fuel injector model and then conducted relevant fault diagnosis research based on the model [20]. Therefore, this paper used Amesim software to model the fuel system and validate it through real experiments. This model was then used to simulate the three common faults (single electronic valve failure, double electronic valve failure and accumulator leakage fault) in the fuel system, so as to provide enough fault sample signals for fault diagnosis.

Commonly, the pressure signals in the fuel injection system are non-liner, non-stationary and complex and entropy is one of the non-stationary dynamics methods which can be used effectively in this field [21]. Examples are approximate entropy (AE) [22], sample entropy (SE) [23], fuzzy entropy (FE) [24] and permutation entropy (PE) [25]. These entropies are used to quantify the irregularity of signals on a single time scale, but cannot analyse information on multiple time scales. In order to overcome this limitation, these entropy algorithms are combined with coarse-grained multi-scale methods and fine composite multi-scale methods. For example, Costa [26] proposed mutiscale entropy (MSE) to measure the complexity of time series at different scales. Li [27] proposed impoved multiscale entropy to detect train axle bearing faults. Wang et al. [28] proposed a novel fault diagnosis method based on generalised composite multiscale weighted permutation entropy, supervised Isomap, and a marine predators algorithm-based support vector machine, to extract the sensitive features of rolling bearings and carry out fault diagnosis. However, MSE only considers the low frequency component of the original sequence and ignores the high frequency component. For the time series with a rich fault information distribution, MSE cannot meet the requirements. In order to extract fault information from the high frequency components in the signal, Jiang et al. [29] introduced the concept of hierarchical entropy (HE). Compared with MSE, HE considers both the low frequency components and high frequency components of the signal, which can provide more comprehensive and accurate time pattern information.

Dispersion entropy (DE) overcomes the shortcomings of AE, SE, FE, and PE, with fast calculation speeds, high stability, and greatly improved anti-noise ability. The literature [30] applied multiscale dispersion entropy (MDE) and refined composite multi-scale dispersion entropy (RCMDE) for the fault diagnosis of rolling bearings, sliding bearings, gearboxes and other rotating machinery, and has achieved

good diagnostic results. However, DE only considers the absoluteness of the amplitude and does not consider the relativity, so it cannot evaluate the fluctuation of the signal. Azami et al. [31] proposed fluctuation-based dispersion entropy (FDE), which is generalised to multiscale fluctuation-based dispersion entropy (MFDE) and refined composite multi-scale fluctuation dispersion entropy (RCMFDE). FDE takes into account the volatility of the time series and is more robust to baseline drift. When under the same parameters, the calculation speed is faster, due to the reduction of all possible dispersion modes [32]. Therefore, the paper presents hierarchical multiscale fluctuation-based dispersion entropy (HMFDE) as a new fault feature extraction, which combines the advantages of HE and MFDE. The feature extracted by HMFDE, as the matrix representation of the original signal, can evaluate the irregularity of the measured pressure signal for each hierarchical layer and at each scale. Compared with the existing fault extraction methods, HMFDE has the following three main advantages. Firstly, HMFDE can extract deeper information in the measured signals, compared with HMDE and MFDE. Secondly, the HMFDE method, without any dimension reduction process, can avoid the loss of structural information. Thirdly, the presented method can be more widely applied to the ME diesel engine, compared to [33].

The paper investigates the effect of different parameter values on the ability of HMFDE to quantify the uncertainty of signals; HMFDE is then used to extract the matrix features of a fuel injection system. Lastly, a support matrix machine (SMM) is used as a classifier to realise fault diagnosis. The rest of the paper is organised as follows: Section 2 presents the HMFDE method, Section 3 determines the optimal parameters of HMFDE, Section 4 illustrates the detailed fault identification steps of the fuel injection system of an ME diesel engine, Section 5 compares the performance of different methods in fuel injection system fault diagnosis and the conclusions are presented in Section 6.

HIERARCHICAL MULTISCALE FLUCTUATION DISPERSION ENTROPY

In this section, HMFDE is proposed to extract deeper information from the signals, as illustrated in Fig. 1. The proposed method mainly consists of three phases: HE is used to decompose the signal into different layers, MSE is then used to decompose every layer at different scales and, finally, FDE is used to calculate the entropy of each node. The detailed calculation process is described below.

FLUCTUATION DISPERSION ENTROPY

For the given time series $X = \{x_1, x_2, \ldots, x_N\}$ with length *N*, the detailed calculation steps of the FDE algorithm are as follows:

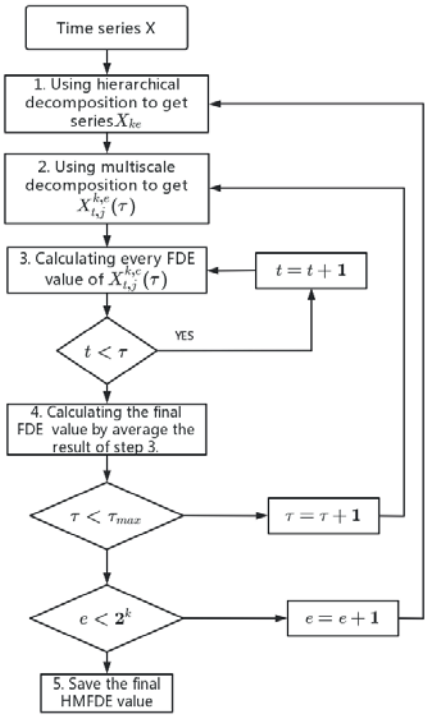

Fig.1. HMFDE flow chart

(1) Xi(i=1~N) is mapped to integer classes ranging from 1 to C by Eq. (1) and (2).

$$Yi = \frac{1}{\sigma\sqrt{2\pi}} \int_{-\infty}^{Xi} \frac{-(t-u)^2}{2\sigma^2} dt \quad (1)$$

$$Zi = R(c * Yi + 0.5) \quad (2)$$

where *u* is expectation, σ is variance, c is an integer and *R* is the rounding function.

(2)The time series Zj can be reconstructed according to the embedding dimension *m* and delay parameter *d*.

$$Zj = \{z_j^c, z_{j+d}^c, \ldots, z_{j+(m-1)*d}^c\}, j=1,2,\ldots, N-(m-1)*d \quad (3)$$

(3) Zj is transformed to a dispersion mode $\pi_{v_0,v_1,\ldots,v_{m-1}}$ and $v_0 = z_j^c$, $v_1 = z_{j+d}^c$,..., v_{m-1}.

(4) The probability of each pattern can be calculated by:

$$p(\pi_{v_0,v_1,\ldots,v_{m-1}}) = \frac{Number(\pi_{v_0,v_1,\ldots,v_{m-1}})}{N-(m-1)*d} \quad (4)$$

(5)The FDE can be calculated by:

$$FDE(X,m,C,d) = -\sum_{\pi=1}^{(2c-1)^{m-1}} p(\pi_{v_0,v_1,\ldots,v_{m-1}}) * \ln(p(\pi_{v_0,v_1,\ldots,v_{m-1}})) \quad (5)$$

FDE takes into account the difference between adjacent elements of the dispersion mode, i.e. the dispersion mode based on fluctuation. In this algorithm, we get a pattern vector with dimension m-1, and each element of the pattern vector ranges from -c+1 to c-1. Therefore, there are $(2c-1)^{m-1}$ wave-based dispersion patterns. When all dispersion patterns have equal probability values, the entropy value is the maximum, which is $\ln[(2c-1)^{m-1}]$. At this time, the signal is completely random.

HIERARCHICAL MULTISCALE DECOMPOSITION

For the given time series X, the hierarchical decomposition process is illustrated in Fig. 2. The detailed calculation steps are as follows:

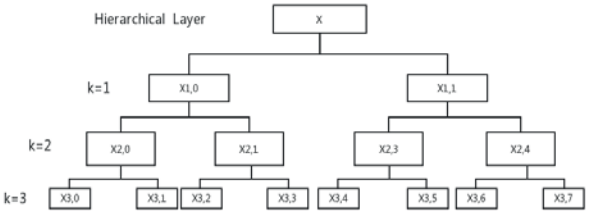

Fig. 2. Hierarchical decomposition process

(1) For a signal X with a length N, define an average operator Q_0 and Q_1 using Eq. (6) and (7); Q_0 represents the low frequency of X and Q_z represents the high frequency of X.

$$Q_0 = \frac{x(2j)+x(2j+1)}{2}, \quad j=0,1,\ldots, 2^{n-1} \tag{6}$$

$$Q_1 = \frac{x(2j)-x(2j+1)}{2}, \quad j=0,1,\ldots, 2^{n-1} \tag{7}$$

(2) In order to describe the hierarchical analysis of the signals, the operator (j=0 or 1) at the hierarchical layer k, is written as:

$$Q_j^k = \begin{bmatrix} \frac{1}{2} & \frac{(-1)^j}{2} & 0 & 0 & \cdots & 0 & 0 \\ 0 & 0 & \frac{1}{2} & \frac{(-1)^j}{2} & \cdots & 0 & 0 \\ 0 & 0 & 0 & 0 & \cdots & \frac{1}{2} & \frac{(-1)^j}{2} \end{bmatrix}_{2^{n-1}*2^n} \tag{8}$$

(3) To obtain the hierarchical components $X_{k,e}$ of each layer in the hierarchical decomposition process, the operator Q_j^k is used repeatedly. At the same time, define the one-dimensional vector $[[\gamma_1, \gamma_2, \cdots, \gamma_n] \in \{0, 1\}]$ and integer

$$e = \sum_{j=1}^{n} \gamma_j 2^{n-j} \tag{9}$$

(4) Based on vector $[\gamma_1, \gamma_2, \cdots, \gamma_n]$, the hierarchical component of the e-th node of the k-th layer can be calculated by

$$X_{k,e} = Q_{\gamma_k}^k \cdot Q_{\gamma_{k-1}}^{k-1} \cdots Q_{\gamma_1}^1 \cdot X \tag{10}$$

(6) For each $X_{k,e}$, the coarse-gain sequence can be calculated by

$$X_{t,j}^{k,e}(\tau) = \frac{1}{\tau}\sum_{i=t+(j-1)\tau}^{t+j\tau-1} X_{k,e}, \ 1 \le j < \frac{L}{\tau}, 1 \le t \le \tau \tag{11}$$

(6) The FDE value of $X_{t,j}^{k,e}$ can be calculated by Eq. (1)-(5) and the HMFDE value can be calculated by

$$\mathrm{HMFDE}(X_{k,e}) = \frac{1}{\tau}\sum_{t=1}^{\tau} FDE(X_{t,j}^{k,e}(\tau)) \tag{12}$$

PARAMETERS OF HMFDE

According to the concept of HMFDE, there are six key parameters which need to be set in advance: the length of the time series N, embedding dimension m, category c, delay time d, hierarchical layer k and scale factor τ. For the hierarchical layer k, if it is too large, it will lead to too few decomposition data points and the calculation efficiency will become low. If the value of k is too small, the frequency band division of the original data will not be detailed enough to fully obtain the frequency band information of the data. According to the relevant literature, the value of hierarchical layer k is set to 3, the scale factor is set to 10 and the delay time is set to 1. In order to evaluate the influence of the remaining parameters, we selected 30 groups white Gaussian noise and 1/f noise as the simulation data. By calculating HMFDE for each group data, the coefficient of variation (CV), consumption time (CT) and Euclidean distance (ED) are used as evaluation indexes of HMFDE stability, and the expressions for CV and ED are shown in Eq. (13) and (14).

$$\mathrm{CV} = \frac{\text{standard deviation}}{\text{mean value}} \tag{13}$$

$$\mathrm{ED} = \sqrt{\sum_{i=1}^{\tau}\sum_{j=1}^{k}(H1(i,j) - H2(i,j))^2} \tag{14}$$

where H1(i,j) and H2(i,j) denote two different HMFDE values

PARAMETER OF DATA LENGTH N

By using the aforementioned method, the matrix characteristics can be extracted and the relevant results are presented in Fig. 3. It can be seen that, with the increase of scale factor, the HMFDE values tend to decrease, which means that the complexity is reduced and is consistent with the actual situation. From Table 2, Table 3 and Table 4, we can conclude that the data length has little influence on the stability of HMFDE. However, with an increase in data length, the average time consumed will increase significantly. After much consideration, a data length of 2048 was chosen.

Tab. 2. Time consumed with different data lengths

Data length	512	1024	2048	4096
White Gaussian noise	0.0330	0.0824	0.2449	0.8063
1/f noise	0.0320	0.0856	0.2499	0.7743

Tab. 3. CV value with different data lengths

Data length	512	1024	2048	4096
White Gaussian noise	0.0325	0.0376	0.0232	0.0214
1/f noise	0.0523	0.0568	0.0571	0.0608

Tab. 4. ED value with different data lengths

Data length	512	1024	2048	4096
ED	1.5804	1.4880	1.7922	2.0630

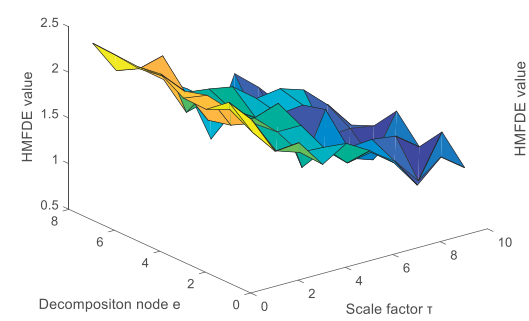

(a) White Gaussian noise with 512 points

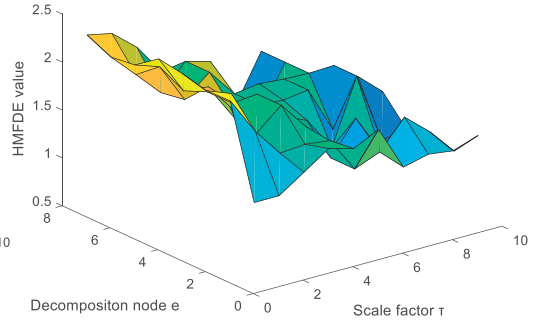

(b) 1/f noise with 512 points

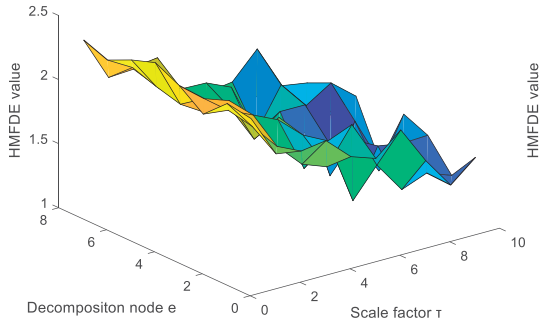

(c) White Gaussian noise with 1024 points

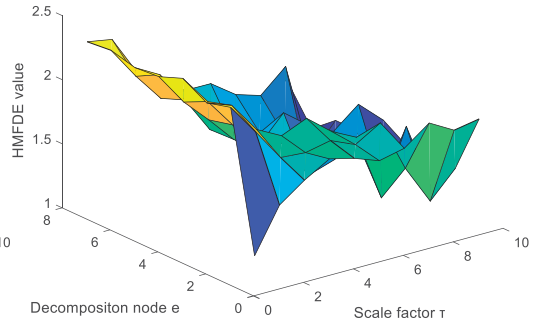

(d) 1/f noise with 1024 points

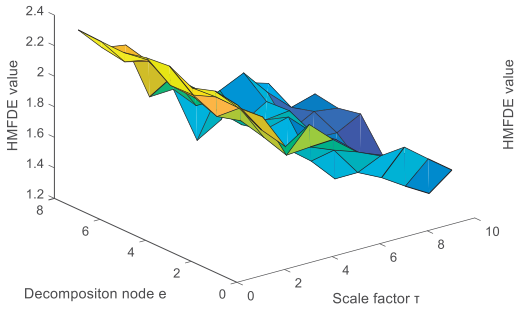

(e) White Gaussian noise with 2048 points

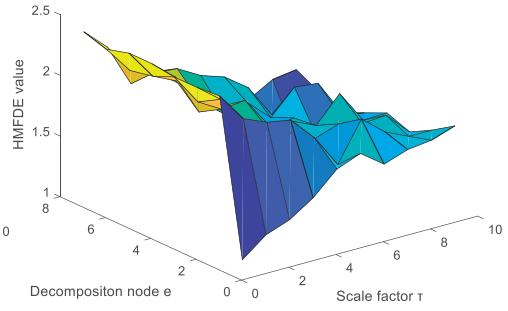

(f) 1/f noise with 2048 points

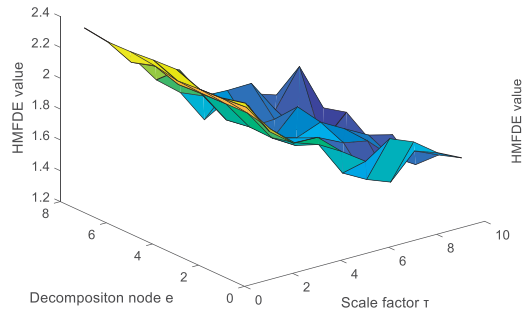

(g) White Gaussian noise with 4096 points

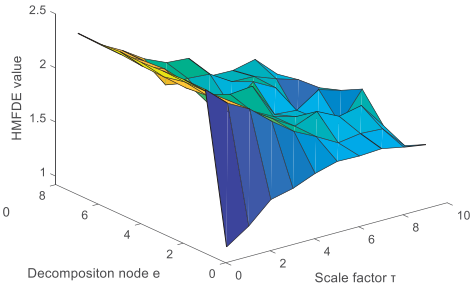

(h) 1/f noise with 4096points

Fig. 3. HMFDE value with different data lengths

PARAMETER OF EMBEDDING DIMENSION M

If the embedding dimension is too small, the dynamic transformation cannot be observed, but if the dimension is too large, a small change cannot be observed. The range of parameters selected in the research was 2-5. From Fig. 4, we can see that, with the increasing embedding dimension, the HMFDE value increases, which means that the complexity is increasing. From Table 5 to Table 7, the time consumption is longer when m is larger than 3; the ED value is at its largest when m is 3, and the CV value is basically the same. So, after comprehensive consideration, an embedding dimension of 3 was chosen in the research.

Tab. 5. Time consumed with different embedding (s)

Embedding	2	3	4	5
White Gaussian noise	0.2414	0.2787	0.3987	1.6804
1/f noise	0.2424	0.2574	0.3903	1.6618

Tab. 6. CV value with different embedding

Embedding	2	3	4	5
White Gaussian noise	0.0232	0.0215	0.0198	0.0125
1/f noise	0.0671	0.0670	0.0624	0.0450

Tab. 7. ED value with different embedding

Embedding	2	3	4	5
ED	1.7922	2.9232	2.8303	1.9596

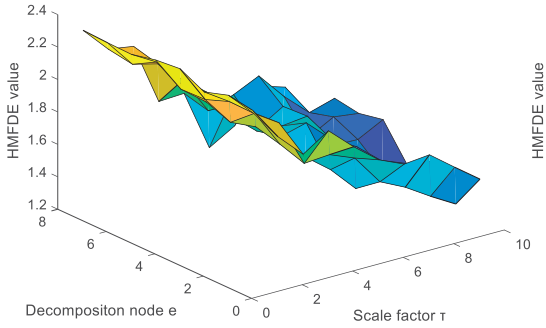

(a) White Gaussian noise with m=2

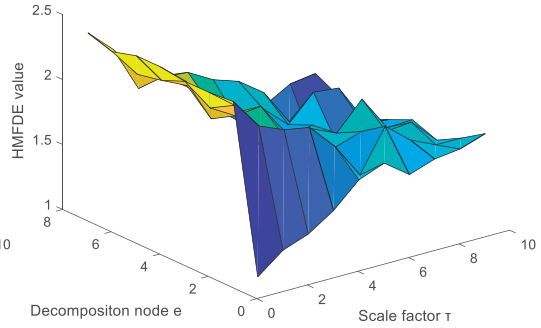

(b) 1/f noise with m=2

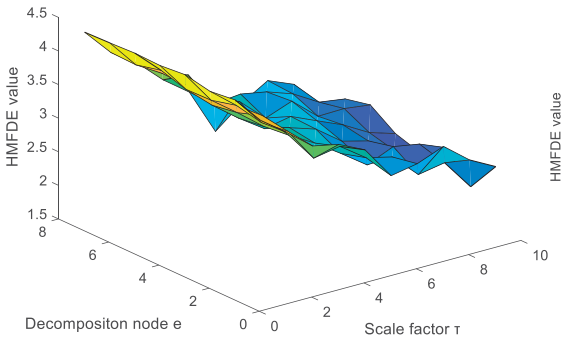

(c) White Gaussian noise with m=3

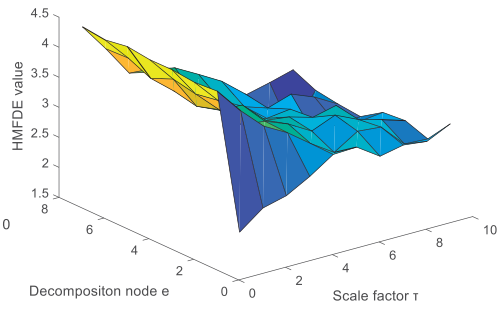

(d) 1/f noise with m=3

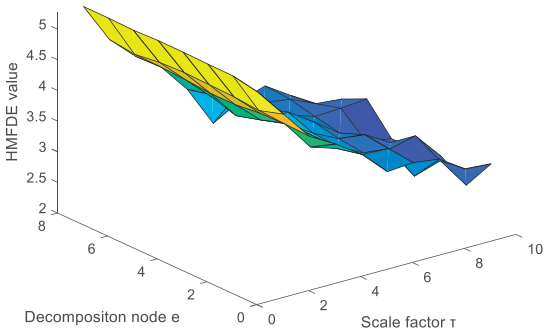

(e) White Gaussian noise with m=4

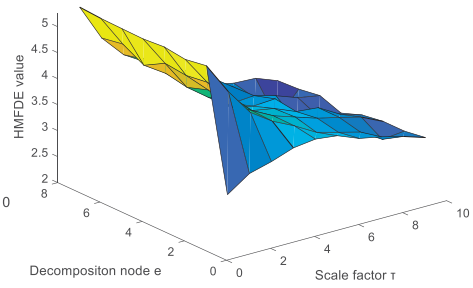

(f) 1/f noise with m=4

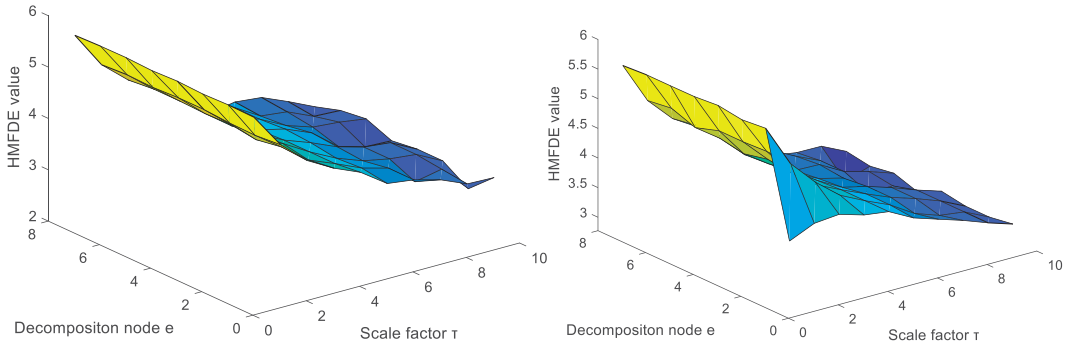

(g) White Gaussian noise with m=5 *(h) 1/f noise with m=5*

Fig. 4. HMFDE value with different embedding m.

PARAMETER OF CATEGORY C

The parameter c is used to balance the entropy value and signal information loss. If the c value is too small, some detailed information may be lost, whereas, if the c value is too large, some subtle amplitude differences may lead to different classifications. Here, we discuss the influence with c ranging from 4-7. Fig. 5, Table 8, Table 9 and Table 10 show that, when c is 6, the HMFDE value is more stable and easier to identify. So, category c was chosen as 6 in the research.

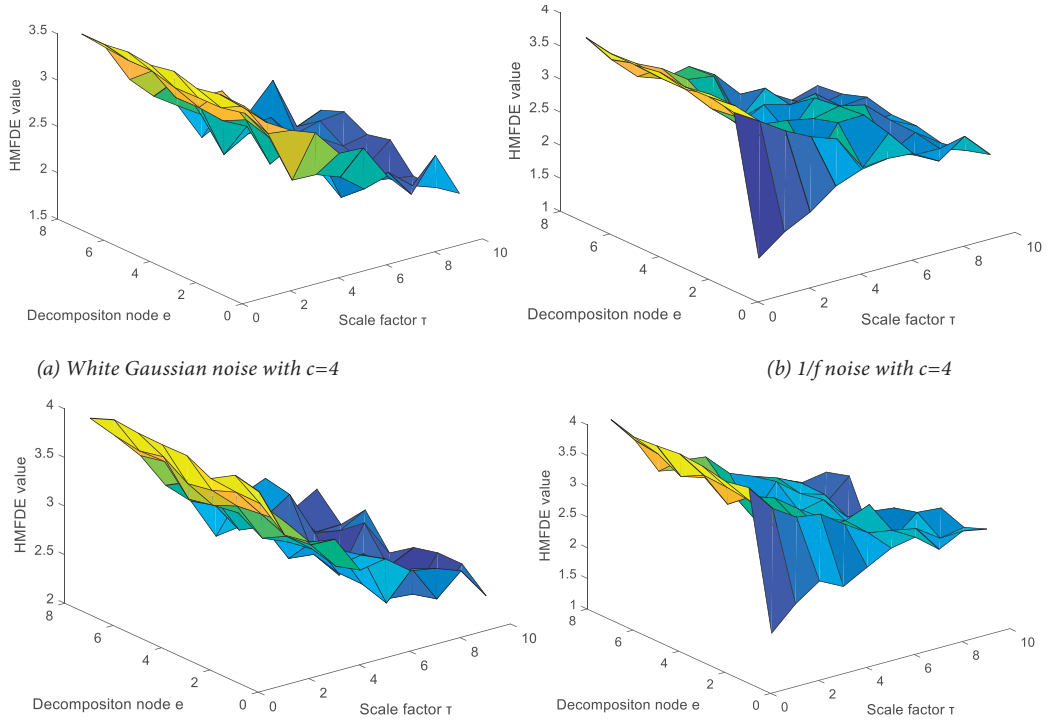

(a) White Gaussian noise with c=4 *(b) 1/f noise with c=4*

(c) White Gaussian noise with c=5 *(d) 1/f noise with c=5*

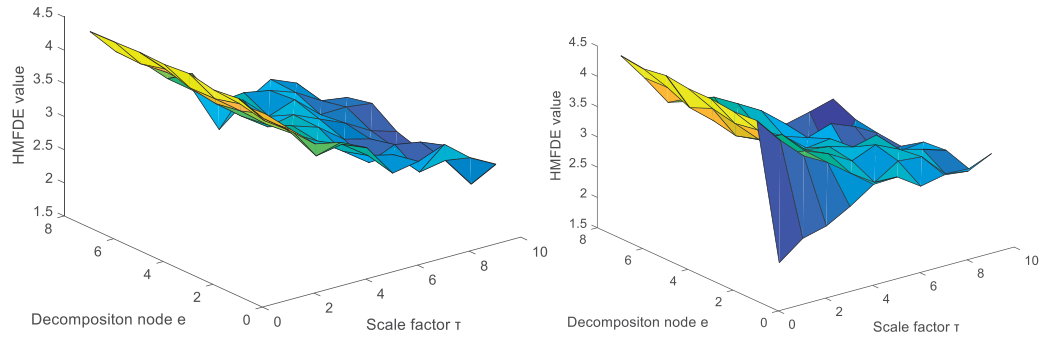

(e) White Gaussian noise with c=6

(f) 1/f noise with c=6

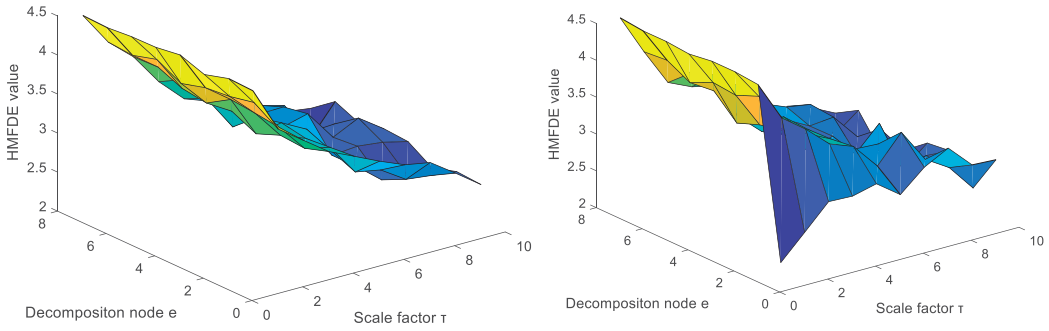

(g) White Gaussian noise with c=7

(h) 1/f noise with c=7

Fig. 5. HMFDE value with different category c

Tab. 8. Time consumed with different category (s)

Category	4	5	6	7
White Gaussian noise	0.2456	0.2547	0.2478	0.2560
1/f noise	0.2662	0.2564	0.2494	0.2544

Tab. 9. CV value with different category

Category	4	5	6	7
White Gaussian noise	0.0254	0.0265	0.0215	0.0143
1/f noise	0.0812	0.0704	0.0680	0.0662

Tab. 10. ED value with different category

Category	2	3	4	5
ED	2.9730	2.9553	2.9632	2.9601

EXPERIMENTAL STUDY

The experimental setup was a two-stroke marine diesel engine in Shanghai Maritime University, which was manufactured by the Diesel Engine Company of MAN B&W 6S35ME-B9. The main parameters of the engine are listed in Table 11. The fuel injection system of the engine mainly consisted of a hydraulic power unit (HPU), a hydraulic cylinder unit (HCU) and an engine control system (ECS). The HPU mainly comprises a filter and hydraulic pumps; its main function being to provide sufficient power for fuel injection and exhaust valve action. The HCU mainly consisted of a fuel injection valve activation (FIVA), an accumulator, a fuel supercharger and an exhaust valve driver; the main function of it is to realise the fuel injection and exhaust valve action of each cylinder. The ECS is the control core of the whole diesel engine, which operates it efficiently and continuously.

Tab. 11. Main technical parameters of the marine diesel engine

Number	Parameter	Value
1	Number of strokes	2
2	Firing sequence	1-5-3-4-2-6
3	Rated power	3570 kW
4	Rated speed	140 r/min
5	Compression ratio	21
6	Cylinder bore/Stroke	350 mm/1550 mm
7	Connecting rod length	1550 mm
8	Intake mode	Supercharging cooling
9	Injection timing	After top dead center (TDC) 2-4°CA

Because it is dangerous and expensive to carry out fault testing on a real marine two-stroke diesel engine, Amesim software was selected to simulate performance. The details of the model can be found in the literature [11-13]. In order to show the picture more clearly, only two fuel injectors are shown here. Fig. 6 shows two super components being used, instead of an axial piston pump. In fact, by using a verified simulation model, we can further analyse and understand the performance of the fuel injection system, comprehensively. First of all, the experiments were carried out on diesel engines with working loads of 100% and the tests lasted 150 minutes. As the fuel oil consumption was more important to guarantee the working

condition of the whole engine, it was calculated every 30 minutes; then this parameter was selected as the simulation model input boundary. The comparison between the simulation and the experimental results is shown in Fig.7. It can be seen that the simulation results almost share the same trend as the experimental results. The MSE (mean-square error) between the simulation and the experimental data is only 1.5103, which proves that the established model can accurately predict the cyclical fuel injection characteristics of the system.

In order to validate the effectiveness of the fault diagnosis algorithm, three common diesel engine faults were simulated on the simulation model, under a 100% working load condition (including a stuck solenoid valve, power failure of a solenoid valve and leakage from the accumulator). The first fault is usually caused by carbon deposition on the valve core, which leads to the reduction of the injector needle valve lift. Here, the valve core lift was reduced by 20%. The second fault is usually caused by the ship's vibration, which will cause the solenoid valve coil to fall off; then the corresponding cylinder of the diesel engine misfires. The third fault is usually caused by a lack of maintenance on the accumulator during long-term operations, which reduces the inhibition of the reflected wave in the fuel injection process. Here, we set the accumulator pressure to leak from 20 MPa to 15 MPa. All of these faults affect the pressure fluctuation in the common rail pipeline of a diesel engine. The simulation results are shown in Fig. 8 but it is difficult to recognise the fault types.

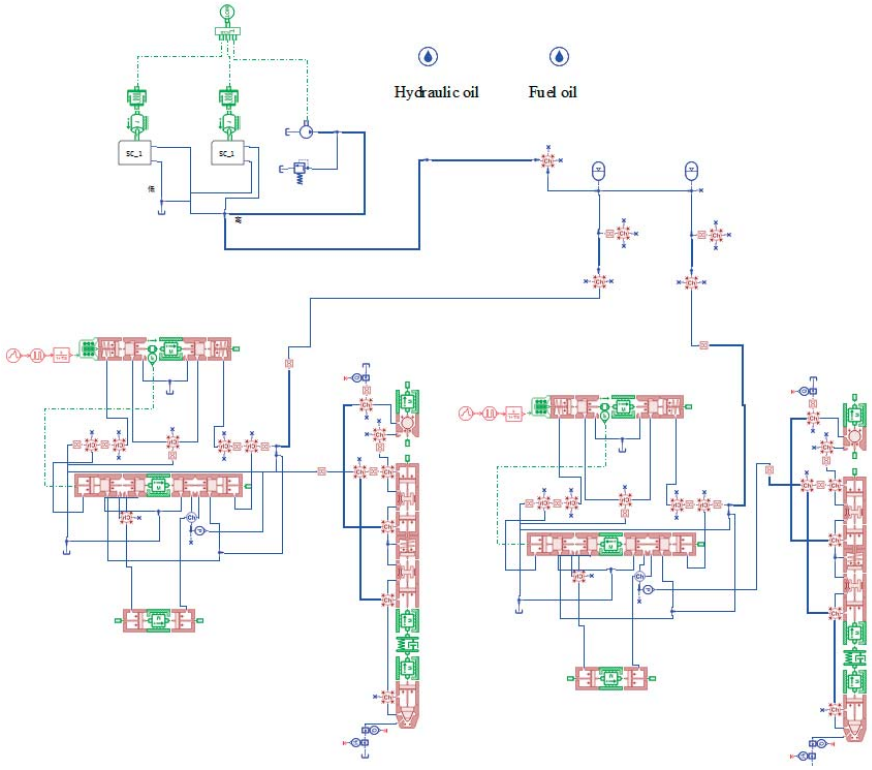

Fig. 6. Amesim model of fuel injection system

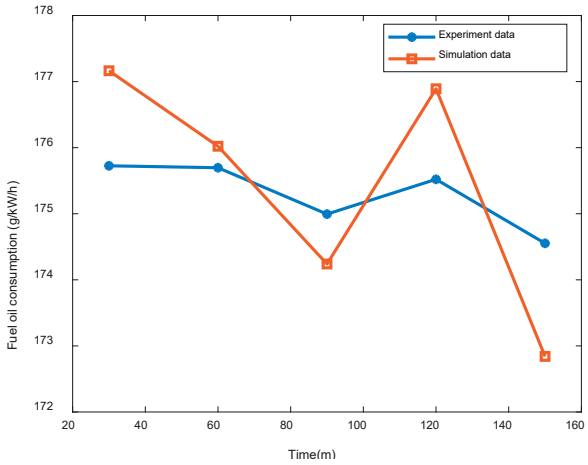

Fig.7. Comparison between experimental and simulation results

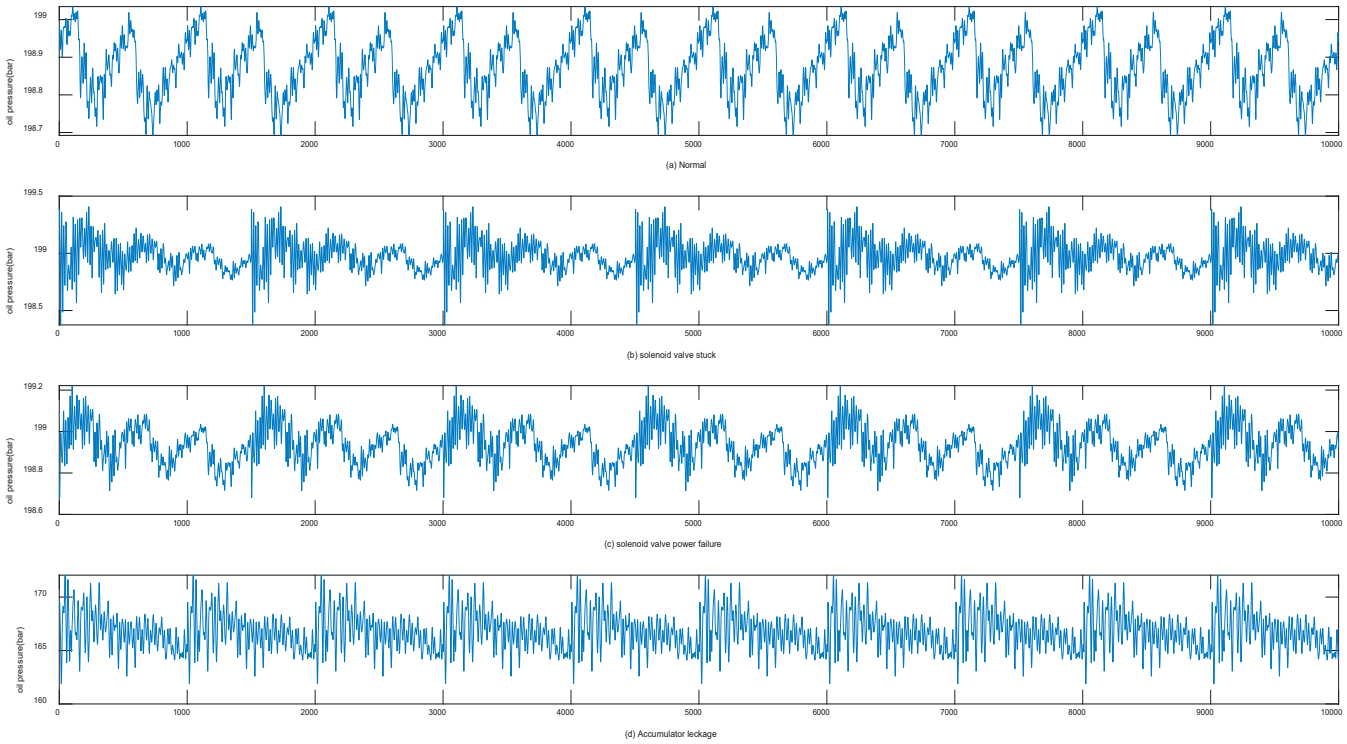

Fig. 8. Fuel pressure waveform under different working conditions

EXPERIMENTAL RESULTS AND ANALYSIS

In this section, the fault diagnosis of an ME fuel injection system uses HMFDE to extract the matrix form features and SMM to realise the classification. The fault diagnosis process is shown as below:

Step 1: The measured signals of different fuel injection fault patterns are collected by simulation and then 20 samples are selected as training data and 30 samples as testing data. Therefore, there are 80 groups of training data and 120 groups of test data, in total.

Step 2: The HMFDE approach is presented to extract fault features directly from the training and testing samples in matrix form.

Step 3: The fault classification algorithm is introduced to build the multiclass SMM, and the HMFDE values of training samples are used for training SMM.

Step 4: The HMFDE values of testing samples are fed into the trained SMM-based binary tree to identify fuel injection system fault patterns.

According to the fault diagnosis method, the proposed feature extraction approach is utilised to extract fault features for each scale and each hierarchical layer from the sample set; the corresponding HMFDE values of different fuel injection system fault patterns are illustrated in Fig. 9. To increase the robustness of classification results, the research randomly selects the HMFDE of 80 training samples under four working conditions, to train SMM, and the optimum model of SMM is estimated. Eventually, the research selects the remaining HMFDE of 120 test samples to validate the effectiveness of the SMM model and the confusion matrix is shown in Fig. 11(a). It can be seen that the accuracy rate reaches 97.5%, there is only one misdiagnosed sample for the 'solenoid valve stuck' working condition and two misdiagnosed samples for the 'solenoid valve power failure' working condition, while other working conditions have been perfectly recognised. This is because both situations have a strong influence on the fuel injection process and cause an increase in the fuel pressure fluctuation of the common rail fuel pipe. When the accumulator leaks, it will only affect the duration of the fuel injection and it has little effect on the action of the injector needle valve.

Then, the matrix characteristic features of HMFDE are vectorised, to verify the validity and rationality of the matrix features. In contrast to this, a support vector machine (SVM) is used as a classifier to recognise the fault types. Comparison tests are conducted eight times and the results are shown in Fig.10. As can be seen from this picture, the combination of HMFDE and SMM has higher fault diagnosis accuracy, with an average of 3 percentage points. This means that the matrix formation has richer information in the HMFDE value.

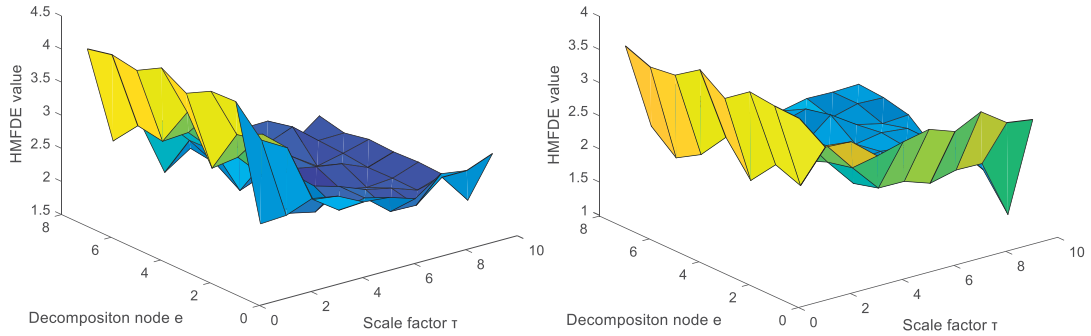

(a) Normal working condition

(b) 'Solenoid valve stuck' condition

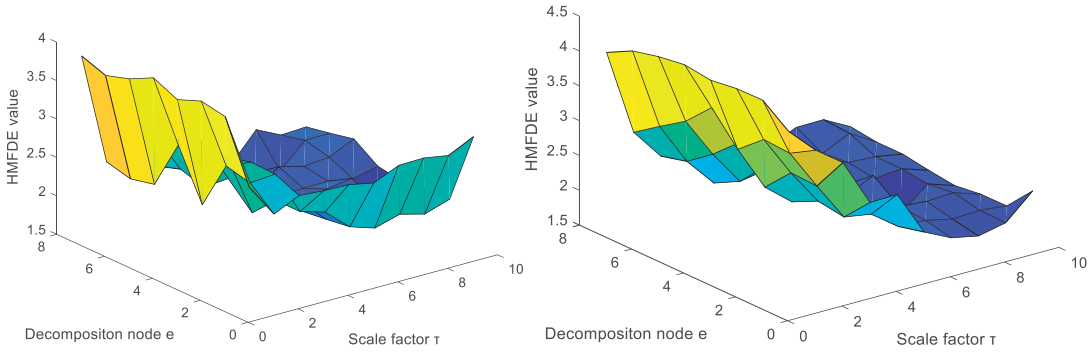

(c) Solenoid valve power failure

(d) Accumulator leakage condition

Fig. 9. HMFDE value of different working conditions.

To further verify the effectiveness of the method, the research also selects the existing entropy-based fault diagnosis method for comparison, e.g. MFDE, HDE, MDE and so on. The detailed parameter settings of these methods are listed in Table 12. The comparison test uses the same training data and testing data, and each method is carried out five times. The average accuracy and time consumed are shown in Table 13. The method proposed in this paper has the highest diagnostic accuracy, while the time consumed is at a relevant low level. Based on the above analysis, it can be verified that HMFDE is superior to the existing common information entropy method, in expressing the complexity of time series; it also verifies the feasibility and superiority of the fuel injection system diagnosis method, based on the HMFDE-SMM method. The confusion matrix of the six methods is shown in Fig. 11. Fault 1 and fault 2 are easily confused, which further explains why a fault with the solenoid valve will have an impact on diesel engine oil pressure in the common rail pipe. However, the influence on pressure varies with the degree of solenoid valve failure. In fact, a solenoid valve failure fault will further lead to power imbalance, exhaust temperature rise, wheelbase wear and other faults in a diesel engine. Therefore, the diagnosis technology can effectively improve the diagnosis efficiency on the fuel injection system of an ME diesel engine, so as to ensure the economic and efficient operation of the whole diesel engine.

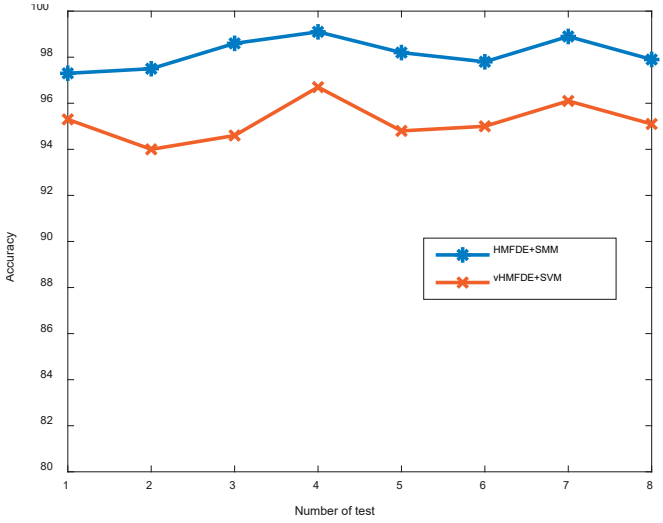

Fig. 10. Accuracy of contrast test

Tab. 12. Parameters of different methods

Method	Classifier	Parameters
HMDE	SMM	k=3,m=3,c=6,τ=1, scale=10
HPE	SVM	k=3,m=3,τ=1
MFDE	SVM	m=3,c=6,τ=1, scale=10
MDE	SVM	m=3,c=6,τ=1, scale=10
MSE	SVM	m=3,scale=10, r=0.1

Tab. 13. Comparison of different methods

Methods	**HMFDE**	**HMDE**	**HPE**	**MDE**	**MFDE**	**MSE**
Accuracy	97.5%	95.8%	86.7%	95.8%	96.7%	91.6%
Consuming time(s)	8.5 s	7.9 s	17.7 s	6.6 s	8.2 s	28.3 s

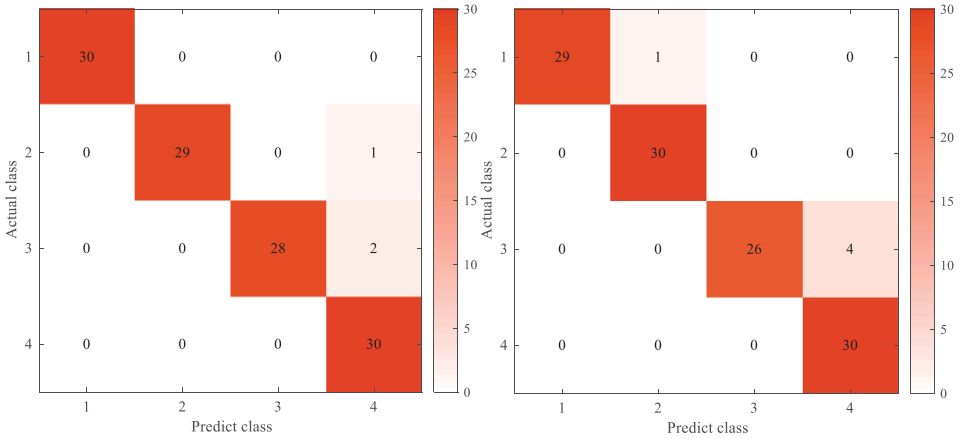

(a) HMFDE

(b) HMDE

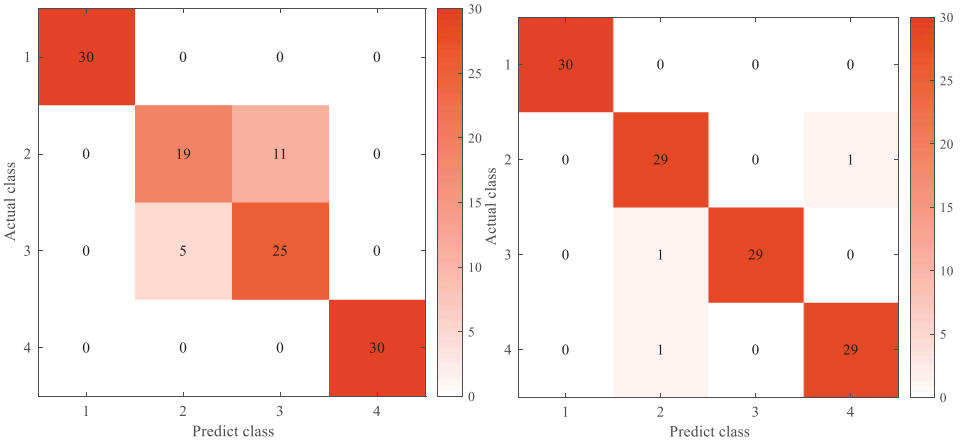

(c) HPE

(d) MFDE

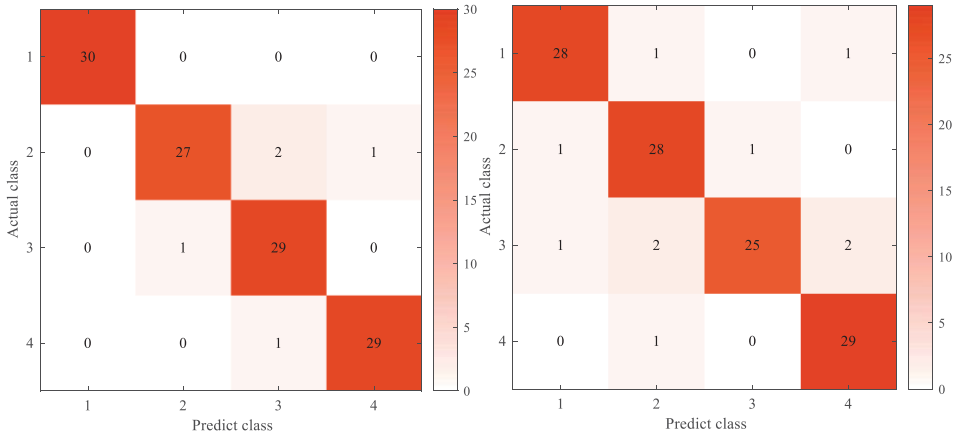

(e) MDE

f) MSE

Fig. 11. Confusion matrix of different methods

CONCLUSION

This paper proposes a novel fault diagnosis method, based on hierarchical HMFDE and SMM, for the fuel injection system of an ME two-stroke diesel engine and the effectiveness of the algorithm is verified by modelling data from the fuel injection system. The paper contributes the following.

1. Through experiment and simulation, the simulation model of the fuel injection system is established, which provides a simple and efficient way for further analysis of the working mechanism.
2. The HMFDE algorithm is proposed, which combines the advantages of HSE and MDE. The influence of parameter variations on calculation accuracy and efficiency is discussed. The method can extract the matrix form features and capture more, hidden fault information.
3. The SMM is used as the classifier. Compared with existing signal classifiers, which are based on vector-form data, the SMM can leverage the inherent structural information of fault signals for more accurate multiclass classification.
4. Compared with HMDE, HPE, MDE, MFDE and MSE, the HMFDE has the highest classification ability, which provides a new way of thinking about the signal complexity evaluation method based on entropy parameters. It also provides a new method for fault diagnosis in an electronically controlled marine two-stroke diesel engine.

ACKNOWLEDGEMENTS

This work was supported by the Science & Technology Commission of Shanghai Municipality and Shanghai Engineering Research Center of Ship Intelligent Maintenance and Energy Efficiency, under Grant 20DZ2252300.

DECLARATION OF COMPETING INTERESTS

The authors declare that they have no known competing financial interests or personal relationships that could have appeared to influence the work reported in this paper.

REFERENCES

1. A. Alahmer, "Influence of using emulsified diesel fuel on the performance and pollutants emitted from diesel engine," Energy Conversion and Management, vol. 73, pp. 361-369, 2013. doi:10.1016/j.enconman.2013.05.012.

2. C.W. Mohd, M.M. Noor and R. Mamat, "Biodiesel as alternative fuel for marine diesel engine applications: A review," Renewable and Sustainable Energy Reviews, vol. 94, pp. 127-142, 2018. doi:10.1016/j.rser.2018.05.031.

3. Z. Korczewski, "Energy and emission quality ranking of newly produced low-sulphur marine fuels," Polish Maritime Research, Vol.21, No.3, pp. 77-87, 2022, doi:10.2478/pomr-2022-0045.

4. J. Blasco, V. Duran-Grados, M. Hampel and J. Moreno, "Towards an integrated environmental risk assessment of emissions from ships' propulsion systems," Environment International, vol. 66, pp. 44-47, 2014, doi:10.1016/j.envint.2014.01.014.

5. K. Rudzki, P. Gomulka and A.T. Hoang, "Optimization model to manage ship fuel consumption and navigation time," Polish Maritime Research, Vol.21, No.3, pp. 141-153, 2022, doi:10.2478/pomr-2022-0034.

6. J. Kowalski, "An experimental study of emission and combustion characteristics of marine diesel engine with fuel injector malfunctions," Polish Maritime Research, Vol.21, No.1, pp. 77-84, 2016, doi:10.1515/pomr-2016-0011.

7. L. Liu, X. Chen, D. Liu, J. Du, and W. Li, "Combustion phase identification for closed-loop combustion control by resonance excitation in marine diesel engines," Mechanical Systems and Signal Processing, vol. 163, pp. 108115, 2022, doi:10.1016/j.ymssp.2021.108115.

8. Y. Bai, L. Fan, X. Ma, H. Peng and E. Song, "Effect of injector parameters on the injection quantity of common rail injection system for diesel engines," International Journal of Automotive Technology, vol. 17, no. 4, pp. 567-579, 2016, doi:10.1007/s12239-016-0057-2.

9. V. Knežević, L. Stazić, J. Orović and Z. Pavin, "Optimisation of reliability and maintenance plan of the high-pressure fuel pump system on marine engine," Polish Maritime Research, Vol.29, No.4, pp. 97-104, 2022, doi:10.2478/pomr-2022-0047.

10. X. Wang, C. Liu, F. Bi, X. Bi and K. Shao, "Fault diagnosis of diesel engine based on adaptive wavelet packets and EEMD-fractal dimension," Mechanical Systems and Signal Processing, vol. 47, pp.581-597, 2013, doi:10.1016/j.ymssp.2013.07.009.

11. K. Tomi, H. Mika and H. Kalevi, "Analysis of common rail pressure signal of dual-fuel large industrial engine for identification of injection duration of pilot diesel injectors," Fuel, vol. 216, pp. 1-9, 2018, doi:10.1016/j.fuel.2017.11.152.

12. Y. Yang, A. Ming, Y. Zhang and Y. Zhu, "Discriminative non-negative matrix factorisation (DNMF) and its application to the fault diagnosis of diesel engine. Mechanical Systems and Signal Processing", vol.95, pp.158-171, 2017, doi:10.1016/j.ymssp.2017.03.026.

13. M. Desbazeille, R.B. Randall, F. Guillet, M. Badaoui and C. Hoisnard, "Model-based diagnosis of large diesel engines based on angular speed variations of the crankshaft," Mechanical Systems and Signal Processing, vol.24, no.5, pp.1529-1541, 2010, doi:10.1016/j.ymssp.2009.12.004.

14. Y. Liu, J. Zhang and L. Ma, "A fault diagnosis approach for diesel engines based on self-adaptive WVD, improved FCBF and PECOC-RVM," Neurocomputing, vol.177, pp. 600-611, 2016, doi:10.1016/j.neucom.2015.11.074.

15. O. Cherednichenko, S. Serbin, M. Tkach, J. Kowalski and D.F. Chen,'Mathematical modelling of marine power plants with thermochemical fuel treatment,' Polish Maritime Research, Vol.29, No.3, pp. 99-108, 2022, doi:10.2478/pomr-2022-0030.

16. R. Varbanets, O. Shumylo, A. Marchenko, D. Minchev, V. Kyrnats, V. Zalozh, N. Aleksandrovska, R. Brusnyk and K. Volovyk, "Concept of vibroacoustic diagnostics of the fuel injection and electronic cylinder lubrication systems of marine diesel engines," Polish Maritime Research, Vol.29, No.4, pp. 88-96, 2022, doi:10.2478/pomr-2022-0046.

17. R. Zhao, L.P. Xu, X.W. Su, S.Q. Feng, C.X. Li, Q.M. Tan and Z.C. Wang, 'A numerical and experimental study of marine hydrogen-natural gas-diesel tri-fuel engines,' Polish Maritime Research, Vol.27, No.4, pp.80-90, 2020, doi:10.2478/pomr-2020-0068.

18. C.G. Rodriguez, M.I. Lamas, J.D. Rodriguez and A. Abbas, "Analysis of the Pre-Injection System of a Marine Diesel Engine Through Multiple-Criteria Decision-Making and Artificial Neural Networks," Polish Maritime Research, Vol. 28, No.4, pp. 88-96, 2021, doi:10.2478/pomr-2021-0051.

19. V.K. Gupta, Z. Zhang and Z. Sun, "Modelling and control of a novel pressure regulation mechanism for common rail fuel injection systems," Applied Mathematical Modelling, vol. 35, pp. 3473–3483.2011, doi:10.1016/j.apm.2011.01.008.

20. H.P. Wang, D. Zheng and Y. Tian, "High pressure common rail injection system modelling and control," ISA Transactions, vol.63, pp.265-273, 2016, doi:10.1016/j.isatra.2016.03.002.

21. Y. Li, X. Wang, Z. Liu, X. Liang and S. Si, "The entropy algorithm and its variants in the fault diagnosis of rotating machinery: a review," IEEE Access, vol. 6, pp.66723–66741, 2018, doi:10.1109/ACCESS.2018.2873782.

22. X. Gao, X. Yan, P. Gao, X. Gao and S. Zhang, "Automatic detection of epileptic seizure based on approximate entropy, recurrence quantification analysis and convolutional neural networks," Artificial Intelligence in Medicine, vol. 102, 101711, 2020, doi:10.1016/j.artmed.2019.101711.

23. J. Zhang, J. Zhang, M. Zhong, J. Zheng and L.Yao, "A GOA-MSVM based strategy to achieve high fault identification accuracy for rotating machinery under different load conditions," Measurement, vol.163, 108067, 2020, doi:10.1016/j.measurement.2020.108067.

24. Z. Jinde, C. Junsheng and Y. Yang, "A rolling bearing fault diagnosis approach based on LCD and fuzzy entropy," Mechanism and Machine, vol.70, pp. 441–453, 2013, doi: 10.1016/j.mechmachtheory.2013.08.014.

25. R. Yan, Y. Liu and R.X. Gao, "Permutation entropy: a nonlinear statistical measure for status characterization of rotary machines," Mechanical Systems and Signal Processing, vol. 29, pp.474–484, 2012, doi:10.1016/j.ymssp.2011.11.022.

26. M. Costa, A.L. Goldberger and C.K. Peng "Multiscale entropy analysis of complex physiologic time series," Physical Review Letters, vol.89, no. 6, pp.705–708, 2002, doi:10.1103/PhysRevLett.89.068102.

27. Y. Li, K.E. Feng, X. Liang and M.J. Zuo, "A fault diagnosis method for planetary gearboxes under non-stationary working conditions using improved VoldKalman filter and multi-scale sample entropy," Journal of Sound and Vibration, vol. 439, pp. 271–286, 2019, doi: 10.1016/j.jsv.2018.09.054.

28. Z. Wang, L. Yao, G. Chen and J. Ding, "Modified multiscale weighted permutation entropy and optimized support vector machine method for rolling bearing fault diagnosis with complex signals," ISA Transactions, vol. 114, pp. 470-484, 2021, doi:10.1016/j.isatra.2020.12.054.

29. Y. Jiang, C. K. Peng and Y. Xu, "Hierarchical entropy analysis for biological signals," Journal of Computational & Applied Mathematics, vol. 236, pp. 728-742, 2011, doi: 10.1016/j.cam.2011.06.007.

30. Y.B. Li, X.H. Liang and Y. Wei, "A method based on refined composite multi-scale symbolic dynamic entropy and ISVM-BT for rotating machinery fault diagnosis," Neurocomputing, vol. 315, pp. 246-260, 2018, doi:10.1016/j.neucom.2018.07.021.

31. H. Azami and J. Escudero, "Amplitude-and fluctuation-based dispersion entropy," Entropy, vol. 20, no.3, 2018, doi:10.3390/e20030210.

32. X. Gan, H. Lu and G. Yang, "Fault diagnosis method for rolling bearings based on composite multiscale fluctuation dispersion entropy," Entropy, vol. 21, no. 3, 2019, doi:10.3390/e21030290.

33. Y. Ke, C. Yao, E. Song, Q. Dong and L. Yang, "An early fault diagnosis method of common-rail injector based on improved CYCBD and hierarchical fluctuation dispersion entropy," Digital Signal Processing, vol. 114, 2021, doi:10.1016/j.dsp.2021.103049.